A Parametric Fracture Mechanics Analysis of a Single Fillet Welded T- Joint

T. Nykänen[1], T. Björk[2] and G. Marquis[3]

[1]Senior Assistant (on leave), Laboratory of Steel Structures and Strength of Materials, Department of Mechanical Engineering, Lappeenranta University of Technology, P.O. Box 20, FIN-53851 Lappeenranta, Finland, e-mail: **timo.nykanen@lut.fi**
[2]Project Manager, Senior Assistant, e-mail: **timo.bjork@lut.fi**
[3]Professor, e-mail: **gary.marquis@lut.fi**

ABSTRACT. *The fatigue behaviour of one-sided fillet welded T-joints has been investigated using plane strain Linear Elastic Fracture Mechanics (LEFM) calculations. A maximum tangential stress criterion with the Paris crack growth law was used to predict the separate growth of a root crack and a toe crack under mixed mode K_I - K_{II} conditions. The effect of weld height, h, plate thickness ratio and crack length, w, at the weld root (the lack of penetration) on the fatigue strength, is studied. The weld flank angle is $\beta = 45^o$. The dimensions are expressed as the terms h/t, w/t and T/t, where t = 25 mm and is the main plate thickness. The base-plate thickness is T. The loads had degrees of bending, DOB, of -1, -1/2, 0, 1/2 and 1, where the DOB is defined as $\Delta\sigma_b/(|\Delta\sigma_m| + |\Delta\sigma_b|)$, where the nominal bending stress range is $\Delta\sigma_b$ and $\Delta\sigma_m$ is the membrane stress range in the main plate.*

INTRODUCTION

The welding process introduces inherent surface crack-like flaws at the weld toe, i.e., along the fusion line. During fatigue loading these flaws play a dominant role and reduce the design stresses to a fraction of those allowed for static loading. Due to these flaws, the initiation stage of fatigue failure is often very short, and these flaws can be conservatively regarded as pre-existing cracks. In normal quality welds, these toe cracks are the most common cause of fatigue failures. Root failure is also possible for welds with partial penetration. The dominant failure mode, i.e., toe crack or root crack, depends on weld size, weld geometry, degree of penetration, and the ratio of axial stress to bending stress.

This work is concerned with the fatigue behaviour of fillet welded T-joints made with a single fillet weld. Geometry is shown in Fig. 1. Such joints are common as corner joints for enclosed sections. Linear elastic fracture mechanics was used to calculate fatigue strength for a range of geometries and loading conditions. In particular, the study considered the curved crack growth path, and the separate growth of toe crack and root cracks. In addition to tensile loading, bending and combined tension/bending

moment loading in both directions were examined for both positive and negative mean stress.
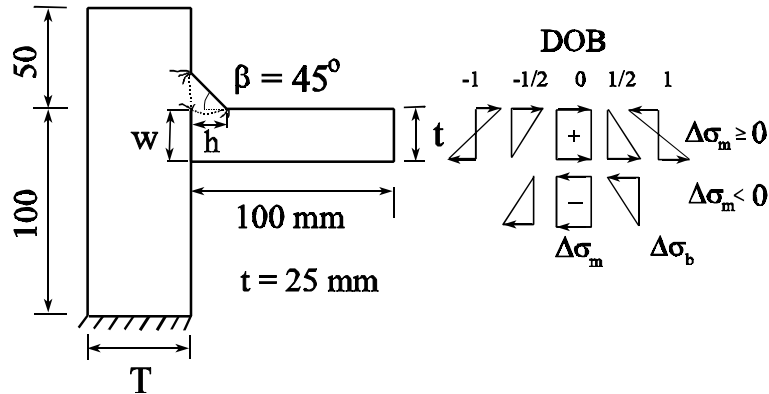

Figure 1. Fillet welded corner.

Referring to Fig.1, for all loading cases the critical crack initiation site is either at the weld toe or at the weld root. The direction of crack growth depends on the type of loading and on the dimensions of the joint. For toe cracks initially perpendicular to the plates, an initial crack length a_i of 0.2 mm was assumed. This length is typical when arc welding is used. A lack of penetration, w, forms the root crack.

MODELS AND METHODS

Loading and Dimensions of the Model
Several finite element analyses were performed with a main plate thickness, t, equals to 25 mm and with a base-plate thickness, T, equals to 25, 37.5 and 50 mm. Eight different cyclic loading combinations of tension and bending were applied at the end of the main plate. The nominal mean stress range was either positive or negative, Fig. 1. These loads had degrees of bending (DOB) of -1, -1/2, 0, 1/2 and 1, where the DOB is defined as $\Delta\sigma_b/(|\Delta\sigma_m| + |\Delta\sigma_b|)$. The nominal bending stress range, $\Delta\sigma_b$, is defined on the lower surface of the main plate in Fig. 1 and $\Delta\sigma_m$ is the membrane stress range in the main plate. Separate crack growth at the weld toe and weld root was assumed. The degree of weld penetration, w, the weld height, h, and the thickness ratio of plates were altered. The analysis was carried out for w/t ratios of 0.008, 0.20, 0.40, 0.70, 1.0, h/t ratios ranging from 0 to 1.25, and T/t ratios ranging from 1.0 to 2.0.

Crack Growth Simulation
The finite element crack growth simulation programme FRANC2D/L by James and Swenson [1] was used in the analysis. The opening mode and sliding mode stress intensity factors K_I and K_{II} were calculated using the J-integral approach (Dodds and Vargas [2]). The influence of K_I and K_{II} on fatigue crack growth is based on the

maximum tangential stress criterion (Erdogan and Sih [3]). Then, the propagation path of the fatigue crack is perpendicular to the maximum principal stress. The same method was applied earlier with reasonable success for different joint types, Nykänen et al. [4,5,6,7,8].

Calculation of Fatigue Life

The fatigue life was calculated using the Paris-Erdogan relation as presented by Gurney [9]. Paris' law for the crack growth rate is

$$\frac{da}{dN} = C \Delta K^m, \tag{1}$$

where da/dN is the crack growth rate per cycle, C and m are constants, and ΔK is the range of the stress intensity factor for the opening mode. The Paris law constants $m = 3$ and $C_{char} = 3 \times 10^{-13}$ ($C_{mean} = 1.7 \times 10^{-13}$), with da/dN in mm/cycle and ΔK in Nmm$^{-3/2}$, are recommended for the analysis of welded steel joints in Hobbacher [10], and are used in this study. The characteristic C_{char}-value given above corresponds to a 95% survival probability. The threshold value of the stress intensity factor was omitted in these simulations. Integrating Eq. 1 so that the variables, i.e., crack length, a, (using a/t instead of a) and number of cycles, N, are separated produces

$$N = \int_{\frac{a_i}{t}}^{\frac{a_f}{t}} \frac{1}{C} \cdot \Delta K^{-m} \cdot t \cdot d\left(\frac{a}{t}\right) = \int_{\frac{a_i}{t}}^{\frac{a_f}{t}} \frac{1}{C} \cdot \left(Y \cdot \Delta \sigma \sqrt{\pi \cdot t \cdot \left(\frac{a}{t}\right)}\right)^{-m} \cdot t \cdot d\left(\frac{a}{t}\right) = \frac{\Delta \sigma^{-m} \cdot I}{C \cdot t^{\frac{m}{2}-1}} \Rightarrow N \cdot \Delta \sigma^m = \frac{I}{C \cdot t^{\frac{m}{2}-1}} \tag{2}$$

where a_i and a_f are the initial and final crack lengths, respectively. The value of the crack growth integral, I, depends on the geometry of the cracked body. In the numerical integration of Esq. 1, which is carried out automatically by the FRANC2D/L program during the crack growth simulation, the final crack length a_{ft} was reached when the increase in fatigue life was negligible.

RESULTS

Mean Fatigue Strength

Several different models were analysed using the simulation program with a certain stress range, $\Delta \sigma$, and thus the mean crack propagation life N was determined. The stress range $\Delta \sigma = *\Delta \sigma_m* + *\Delta \sigma_b*$ was then changed with Eq. 2 to correspond to a fatigue life of two million cycles. Some of the predicted mean fatigue strengths, $\Delta \sigma_{mean}$, are presented in Table 1.

Theoretical Fatigue Class

Using the $\Delta \sigma_{mean}$-values given in Table 1 and $C_{char} = 3 \times 10^{-13}$, the theoretical fatigue class (FAT) for each case analysed can be determined. From Eq. 2, we can obtain the following Eq. 3 for the FAT:

$$FAT = \Delta\sigma_{char} = \sqrt[3]{\frac{C_{mean}}{C_{char}}}\,\Delta\sigma_{mean} = 0.8275\,x\,\Delta\sigma_{mean} \tag{3}$$

with da/dN in mm/cycle and ΔK in Nmm$^{-3/2}$. (For high quality welds, the use of $C_{char} = 2.2 \times 10^{-13}$ might be justified, but for very poor quality welds $C_{char} = 5.4 \times 10^{-13}$, Niemi [11], giving FAT = $0.9176 \times \Delta\sigma_{mean}$ and FAT = $0.6803 \times \Delta\sigma_{mean}$, respectively.)

Table 1. Mean fatigue strengths $\Delta\sigma_{mean}$ (MPa), $N = 2 \times 10^6$.

			Only root crack				Only toe cracks, $a_i = 0.2$ mm					
			DOB, $\Delta\sigma_m \geq 0$				DOB, $\Delta\sigma_m \geq 0$			DOB, $\Delta\sigma_m < 0$		
w/t	T/t	h/t	-1/2	0	1/2	1	-1	-1/2	0	-1/2	0	1/2
0.20	1.0	0.0	183.7	32.7	39.8	52.2	74.3	88.4	111.2	-	-	-
		0.25	151.8	32.7	42.0	61.3	69.8	80.9	97.3	-	-	-
		0.50	125.5	33.5	45.6	86.2	75.8	83.4	95.1	-	-	-
		0.75	113.2	34.2	49.7	80.4	84.8	89.6	96.9	-	-	-
		1.25	103.2	36.8	57.0	80.9	94.5	95.1	103.2	-	-	-
	1.5	0.0	174.4	32.2	40.2	53.7	70.5	82.4	103.2	-	-	-
		0.25	140.9	32.4	42.5	63.0	68.7	81.4	101.3	-	-	-
		0.50	117.6	33.0	46.7	79.9	76.5	85.3	98.6	-	-	-
		0.75	106.6	34.5	51.4	104.5	85.3	91.5	99.3	-	-	-
		1.25	100.7	37.8	61.0	174.4	94.7	95.8	98.6	-	-	-
	2.0	0.0	165.1	31.9	40.4	54.3	69.1	80.2	99.0	-	-	-
		0.25	133.9	32.2	42.7	63.4	68.7	81.4	103.5	-	-	-
		0.50	113.2	33.2	48.6	80.4	76.6	86.2	101.3	-	-	-
		0.75	103.2	34.8	52.2	105.1	85.7	90.5	100.7	-	-	-
		1.25	99.7	38.5	63.0	173.8	96.5	96.7	99.3	-	-	-

THICKNESS EFFECT

The main causes of the observed thickness effect are the technological effect, the statistical effect and the stress gradient effect. The statistical and stress gradient effects are the main factors regarding size effects in welded joints (Örjasäter [12]). The reason for the stress gradient effect is that a crack at the surface of a thick specimen will grow at a higher stress than a crack of the same length in a thin specimen for the same stress at the surface. Thus, the thinner specimen will have a longer fatigue life. For proportionally scaled joints, when the crack is scaled in the same proportion as the other dimensions, the geometrical thickness effect exponent n is -1/6 (when $m = 3$) in Eq. 4 [4] and can be used for root crack case. Eq. 4 is easily derived from Eq. 2.

$$\frac{\Delta\sigma}{\Delta\sigma_0} = \left(\frac{t}{t_0}\right)^{\frac{1}{m}-\frac{1}{2}} = \left(\frac{t}{t_0}\right)^n \tag{4}$$

In Eq. 4 $\Delta\sigma_0$ is the reference fatigue stress range for the reference thickness t_0. So, this geometrical size effect can be calculated using fracture mechanical models.

Scaling the joints proportionally and keeping the initial crack depth at the weld toe constant, i.e., $a_i = 0.2$ mm, the exponent, n, is no more constant. The geometrical thickness effect is dependent on the DOB and the dimension ratios as shown in [7,8]. On the basis of experimental results, a general thickness correction of $n = -1/3$ is proposed by Örjasäter [12]. The value of n depends on the severity of the stress concentration of the joint. For the joints with severe stress concentration like tubular joints in plane bending the exponent is changed to $n = -0.4$ [12]. Because no calculated or test data is available for the joint type studied, the use of the commonly used 'fourth root rule' thickness correction formula, where n equals to -1/4 or the use of more conservative value of $n = -1/3$ when $t = 25$ mm might be justifiable.

However, we can get the theoretical upper and lower bond results for the stress gradient effect in non-proportional case (a_i = constant) using Eq. 2. First we get (when $m = 3$)

$$\frac{\Delta\sigma}{\Delta\sigma_0} = \left(\frac{t}{t_0}\right)^{-\frac{1}{6}}\left(\frac{I}{I_0}\right)^{\frac{1}{3}}. \tag{5}$$

By noting, that if $t \geq t_0$, then $I \geq I_0$ and the lower bound is $\dfrac{\Delta\sigma}{\Delta\sigma_0} = \left(\dfrac{t}{t_0}\right)^{-\frac{1}{6}}$.

If $t < t_0$, then $I < I_0$ and the upper bound is $\dfrac{\Delta\sigma}{\Delta\sigma_0} = \left(\dfrac{t}{t_0}\right)^{-\frac{1}{6}}$. I_0 is the reference crack growth integral for the reference thickness t_0.

ANALYSIS OF RESULTS

The calculations predict the separate growth of a root crack and a toe crack. Because the interaction effect of cracks is insignificant when the cracks are far away from each other, we can merge the separate results in order to get the mean fatigue strength for combined growth of root and toe cracks.

In "as welded" condition the whole stress intensity factor range is regarded as effective. However, for example the root crack in case of DOB = -1 or the toe crack in case of DOB = 1 does not grow in the simulation model because of the local compression-to-compression stresses are keeping the crack closed. In practice, there may exist high tensile residual stresses or reaction stresses at the vicinity of the crack tip if the structure is highly redundant. These residual stresses keep the crack tip open during the stress cycle. The fatigue behaviour can then be expressed in terms of stress range alone [9]. To take the compression-to-compression loading into account, we may define the fatigue strengths corresponding to different DOBs as $\Delta\sigma_{mean}(\text{DOB} = \pm1) = \min\{\Delta\sigma_{mean}(\text{DOB} = -1, \Delta\sigma_m \geq 0), \Delta\sigma_{mean}(\text{DOB} = -1, \Delta\sigma_m < 0), \Delta\sigma_{mean}(\text{DOB} = 1, \Delta\sigma_m \geq 0), \Delta\sigma_{mean}(\text{DOB} = 1, \Delta\sigma_m < 0)\}$, $\Delta\sigma_{mean}(\text{DOB} = 0) = \min\{\Delta\sigma_{mean}(\text{DOB} = 0, \Delta\sigma_m \geq 0),$

$\Delta\sigma_{mean}$(DOB = 0, $\Delta\sigma_m$ < 0)}, $\Delta\sigma_{mean}$(DOB = -1/2, $\Delta\sigma_m \geq 0$) = min{$\Delta\sigma_{mean}$(DOB = -1/2 ,$\Delta\sigma_m \geq$ 0), $\Delta\sigma_{mean}$(DOB = 1/2, $\Delta\sigma_m$ < 0)}, $\Delta\sigma_{mean}$(DOB = 1/2, $\Delta\sigma_m \geq$ 0) = min{$\Delta\sigma_{mean}$(DOB = 1/2, $\Delta\sigma_m \geq$ 0), $\Delta\sigma_{mean}$(DOB = -1/2, $\Delta\sigma_m$ < 0)}, $\Delta\sigma_{mean}$(DOB = -1/2, $\Delta\sigma_m$ < 0) = $\Delta\sigma_{mean}$(DOB = 1/2, $\Delta\sigma_m \geq$ 0) and $\Delta\sigma_{mean}$(DOB = 1/2, $\Delta\sigma_m$ < 0) = $\Delta\sigma_{mean}$(DOB = -1/2, $\Delta\sigma_m \geq$ 0). This definition means that the compressive load cycle is as damaging as the tensile load cycle if in both cases the corresponding nominal stress distributions of stress ranges are the same but opposite. On this way predicted mean fatigue strengths, $\Delta\sigma_{mean}$, in "as welded" condition are presented as 3D graphs in Fig. 2, when T/t = 1 and t = 25 mm.

On the basis of all predicted mean fatigue strengths in "as welded condition", the theoretical fatigue classes were calculated, Eq. 3, and curve fitted using non-linear regression analysis with 3rd degree polynomial, Eq. 6.

$$FAT_{DOB} = \sum_{i=1}^{20} A_{DOB,i} \left(\frac{h}{t}\right)^{a_i} \left(\frac{w}{t}\right)^{b_i} \left(\frac{T}{t}\right)^{c_i} f(t) \tag{6}$$

The theoretical thickness effect correction factor, $f(t)$, is also included in Eq. 6. It is conservatively assumed, that $f(t) = \left(\dfrac{t}{25}\right)^{-\frac{1}{6}}$, when $t \geq$ 25 mm and $f(t) = 1$, when $t <$ 25 mm. The coefficients $A_{DOB,i}$ corresponding to the certain DOB and exponents a_i, b_i and c_i are presented in Table 2, when $\Delta\sigma_m \geq$ 0. If $\Delta\sigma_m <$ 0, then $A_{1/2,i} = A_{-1/2,i}$ and $A_{-1/2,i} = A_{1/2,I}$, where the in both equation the later terms are the coefficients for $\Delta\sigma_m \geq$ 0.
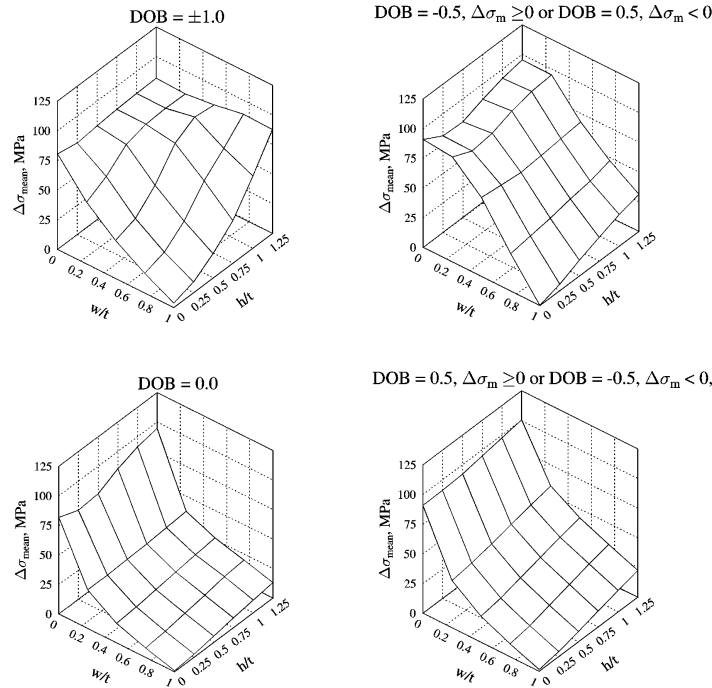

Figure 2. Predicted mean fatigue strength, $\Delta\sigma_{mean}$ (N = 2×10^6 cycles), in "as-welded" condition, T/t = 1 and t = 25 mm.

Table 2. The curve fitted coefficients $A_{DOB,i}$ and exponents a_i, b_i and c_i in Eq 6, when $\Delta\sigma_m \geq 0$.

i	1	2	3	4	5	6	7	8	9	10
$A_{0,i}$	4.01	-7.71	33.04	-144.2	7.35	-33.20	64.45	192.5	-17.68	-0.438
$A_{\pm1,i}$	-3.27	11.78	-2.25	-0.22	-4.11	12.66	-55.80	23.57	8.90	4.96
$A_{0.5,i}$	-2.18	-3.18	-3.00	16.76	-4.48	-18.71	34.67	-35.73	8.61	1.80
$A_{-0.5,i}$	-3.1	-2.72	-45.67	208.1	-7.63	-6.23	20.86	-311	21.16	-4.03
a_i	1	0	0	0	1	0	0	0	1	2
b_i	0	1	0	0	1	2	1	0	0	0
c_i	2	2	3	2	1	1	1	1	1	1

i	11	12	13	14	15	16	17	18	19	20
$A_{0,i}$	-21.27	-116.6	315.1	-286.7	18.98	-2.44	-15.89	8.88	10.51	-2.99
$A_{\pm1,i}$	-106.0	12.50	27.55	-73.99	103.8	38.10	44.87	-10.00	25.23	-22.71
$A_{0.5,i}$	-24.95	-107.8	285.6	-264.0	33.07	0.378	95.44	-8.30	12.63	-6.29
$A_{-0.5,i}$	11.15	234.7	-365.0	46.54	16.57	-6.56	220.6	-42.27	48.66	-17.64
a_i	1	0	0	0	1	2	0	1	2	3
b_i	2	3	2	1	1	1	0	0	0	0
c_i	0	0	0	0	0	0	0	0	0	0

DISCUSSION AND CONCLUSIONS

The fatigue behaviour of one-sided partially penetrating butt weld in corner was investigated by using the 2D linear elastic fracture mechanics calculations. The J-integral method, maximum tangential stress criterion, and Paris' crack growth law were used to predict the fatigue strength. It was assumed that the fatigue life of the joint could be described by the propagation of pre-existing straight-fronted cracks. The initiation period, the semi-elliptic crack-front shape of an initial fatigue crack and the threshold value of stress intensity factor were not taken into account. The whole stress range was assumed to be effective. This should lead to conservative fatigue strength estimates. An initial crack depth of 0.2 mm was assumed for the toe cracks. In finite element model the main plate is free to bend inside the base plate. This should take into account the effect of possible small cap between the plates. Identical fatigue behaviour was assumed for both the weld metal and the parent material. On the basis of these assumptions and fracture mechanics analyses, the following conclusions can be drawn:
(1) Theoretical fatigue strength values for the weld root crack length to plate thickness ratios of $w/t = 0.008 - 1.0$, for weld height to plate thickness ratios of $h/t = 0 - 1.25$, and for base plate thickness to main plate thickness ratios of $T/t = 1.0 - 2.0$ were calculated. The load condition was varied from pure tension loading to pure bending loading and to the combined tension/bending moment loading. Both bending directions were analysed for $\Delta\sigma_m \geq 0$ and for $\Delta\sigma_m < 0$.

(2) Parametric theoretical fatigue class equation for the joint in "as welded" condition was established.

(3) Theoretical lower bond equation for the stress gradient effect in non-proportional case (a_i = constant) was proposed.

(4) The fatigue strength increases with decreasing values of w/t and with increasing values of h/t.

(5) With small w/t-ratios (w/t < 0.2) the fatigue strength of root crack increases when T/t-ratio decreases. When both h/t-ratio and w/t-ratio increase the fatigue strength of toe crack increases with decreasing T/t-ratio. In both cases the rate of change depends on DOB.

(6) The fatigue strength of combined tension and bending cannot be interpolated linearly from the results of pure tension and pure bending. This is because of different crack growth paths and because of different crack initiation points.

REFERENCES

1. James, M. and Swenson, D. "FRANC2D/L: A Crack Propagation Simulator for Plane Layered Structures," available from http://www.mne.ksu.edu/~franc2d/.
2. Dodds, R. H. and Vargas, P. M. (1988) Numerical evaluation of domain and contour integral for non-linear fracture mechanics: formulation and implementation aspects. Report from University of Illinois at Urbana-Champaign, Dept. of Civil Engineering.
3. Erdogan, F. and Sih, G. C. (1963) *ASME J Basic Engng* 85, 519-527.
4. Nykänen, T. (1995) IIW Doc. XIII-1583-95.
5. Nykänen, T. (1996) IIW Doc. XIII-1624-96.
6. Nykänen, T. (1999) IIS/IIW-1432-98. *Welding in the World* **43**, no. 5, 42-46.
7. Nykänen, T. (1999) IIS/IIW-1433-98. *Welding in the World* **43**, no. 5, 47-53.
8. Nykänen, T. and Lihavainen, V-M. (2000) IIW Doc. XIII-1838-2000.
9. Gurney, T. R. (1979) *Fatigue of welded structures*. The Welding Institute, Cambridge University Press, Cambridge.
10. Hobbacher, A. (1996) IIW Doc. XIII-1539-96/XV-845-96.
11. Personal communications with Professor E. Niemi (1993) Lappeenranta University of Technology, Finland.
12. Örjasäter, O. (1993) IIW- JWG XIII-XV-118-93.